Crystallization Behavior and Foaming Properties of Polypropylene Containing Ultra-High Molecular Weight Polyethylene Under Supercritical Carbondioxide

Chunling Xin,[1] Yadong He,[1] Qingchun Li,[1] Yingzhu Huang,[1] Baorui Yan,[1] Xiaodong Wang[2]

[1]*School of Mechanical and Electrical Engineering, Beijing University of Chemical Technology, Beijing 100029, People's Republic of China*
[2]*School of Materials Science and Engineering, Beijing University of Chemical Technology, Beijing 100029, People's Republic of China*

Received 23 December 2008; accepted 7 May 2009
DOI 10.1002/app.30717
Published online 18 August 2010 in Wiley Online Library (wileyonlinelibrary.com).

ABSTRACT: In this study, a systematic investigation on the nonisothermal crystallization kinetics of conversional polypropylene (PP) containing various amounts of ultra-high molecular weight polyethylene (UHMWPE) was reported, and the effects of UHMWPE on crystallization behavior of these PP materials and their foaming properties were also presented. The kinetic studies revealed that the incorporation of UHMWPE into PP led to an increase in the crystallization temperature and temperature range during the crystallization process as well as the relative crystallinity. This behavior was attributed to a comprehensive effect of the nucleation and entanglement of the UHMWPE chains. The kinetic models based on Ozawa's and Mo's methods were used to analyze the nonisothermal crystallization behaviors. It was found that the latter succeeded in describing the nonisothermal crystallization behavior of the PP containing UHMWPE, while the former was not appropriate. The activation energy for the nonisothermal crystallization determined by Kissinger's method also indicated that the crystallization ability of PP was improved with the addition of UHMWPE. Owing to the modification of the crystallization kinetics of the PP materials by introduction of UHMWPE, the foaming properties (i.e., cell uniformity and expandability etc.) were improved significantly. © 2010 Wiley Periodicals, Inc. J Appl Polym Sci 119: 1275–1286, 2011

Key words: PP; UHMWPE; foams; nonisothermal crystallization behavior; foaming properties

INTRODUCTION

Foamed thermoplastics are polymeric materials with a cellular structure created by the expansion of blowing agent. Owing to the presence of numerous voids or cells dispersed throughout their mass, these polymers are characterized by a decreased apparent density and have great advantages such as reduced weight, energy absorption, and low thermal conductivity. This internal structure also achieves an optimization of stiffness, strength, or energy absorption for a given weight, and provides unique properties of the formed plastics for their effective and various industrial applications.[1] The most common polymers used for thermoplastic foams are polystyrene (PS), polyethylene (PE), and polyvinyl chloride. They have advantages of low cost, good temperature stability, high chemical resistance, and wide processing window. Their foamed products have been commercialized for a long time. However, these polymers have limited physical properties, which results in a hindrance to application of their foams.[2]

Polypropylene (PP) is considered to be a substitute of other thermoplastics as foam materials because it has more advantages than PS and PE. PP has a higher rigidity, higher service temperature range, and good temperature stability as compared with other polyolefins, and offers a higher strength and better impact toughness as compared with PE and PS, respectively.[3,4] However, only a few researches have been conducted on the production of PP foams so far, which shows that it is difficult for PP to be foamed for two main reasons: (1) PP is a semi-crystalline polymer with fast crystallization, and it is difficult to form a fine cellular structure in PP in such a narrow processing window; (2) The melt strength of linear PP is very weak. In this case, the cell-separated walls may not have enough strength to bear the extensional force and easily rupture during foaming.[5,6]

Some researches have been conducted to enhance the melt strength and foamability of PP in the last decade. Earlier efforts including the crosslinking and

Correspondence to: X. Wang (wangxdfox@yahoo.com.cn) and Y. He (heyd@mail.buct.edu.cn).

Contract grant sponsor: Tianjin Nature Science Foundation; contract grant number: 08JCYBJC09800.
Contract grant sponsor: The National Key Technology R&D Program for the 11th Five-year Plan; contract grant number: 2008BAE59B04.
Contract grant sponsor: The Municipal Nature Science Foundation of Beijing; contract grant number: 2093041.

blending modification for PP resins significantly improved the volume expandability, cell uniformity, and formability.[7,8] Other efforts have also been made to improve the melt strength of PP materials with long-chain branching.[9,10] Several commercial long-chain branched PP materials with high melt strength have been developed as a foamable grade. Some investigations on foaming mechanism and processing technology were also conducted, but few about the effects of crystallization behaviors of PP resins on formability.[11,12] The crystallization behavior of semicrystalline materials is a critical factor for plastic foam processing. In a typical extrusion foaming process, the melt temperature decreases due to the external cooling outside the foaming die and the cooling effect resulted from isentropic expansion of the blowing gasses. Thus, the processing temperature at the final stage determines the time required for the polymer melt to solidify. For semicrystalline polymers, it was observed that the polymer melt solidifies at the moment of crystallization. Therefore, the foam structure "freezes" at the crystallization temperature, which will make the cells grow to the point, where the foam cannot be fully expanded.[13,14] Besides the effects of the processing parameters on the crystallization, the materials' properties and foaming additives can also contribute to the changes in crystallization temperatures.[15] To obtain good foaming products (fine bubble size and high content of closed cells) from such semicrystalline PP, solutions of polymer/gas system should be cooled as closely as possible to its incept crystallized temperature to enhance the melt viscosity and shorten the solidification time. However, when the temperature approaches to the crystallization temperature, the viscosity of PP will increase sharply due to its intrinsic crystallinity and hence block the growth of bubble definitely.[16,17] On the contrary, if the foaming process is carried out at an elevated temperature, the low viscosity, long crystallization time, and increased probability of gas escape will make it very difficult to prepare PP foams with high folds of expansion.[18] Therefore, the appropriate temperature and crystallization speed play key roles on the stable extrusion foaming of PP materials.[19,20]

Ultra-high molecular weight polyethylene (UHMWPE) is one of the leading plastics that have been developed in recent decades. The outstanding properties of UHMWPE, such as toughness, high wear strength, and abrasion resistance, provide not only new utilities but also scientific interests. UHMWPE has been widely used to optimize the property of polymers such as PE, PP, ethylene-propylene-diene elastomer rubber, polyaniline, and polyacrylate.[21–25] Kayama and coworker[26,27] reported a study on rheology of PP containing small amounts of UHMWPE, and they found that the rheological behavior of the modified PP changed dramatically in comparison with conversional PP. At a low frequency, the melt elasticity increases evidently with longer relaxation time. Wang et al.[28] found that addition of small amount UHMWPE improved the toughness of the PP, which was attributed to the network of UHMWPE domains formed in the PP matrix. Li et al. compared the mechanical properties and morphology of the PP/UHMWPE blends by the injection-compression molding, and found that the injection-molded sample exhibited the higher modulus and yield strength, but the lower toughness and elongation at break, due to the high orientation of UHMWPE particles in the skin part.[29] They also found that the addition of poly(ethylene glycol) could result in a significant reduction of melt viscosity for PP/UHMWPE due to disentanglement effect.[30] Khaira and coworkers[31] developed a novel modification method for PP/PET blends by incorporation of UHMWPE, and the mechanical properties and abrasive wear of these blends could be significantly enhanced. In addition, incorporation of small amount of UHMWPE into PP improved the melt viscosity, and the materials exhibited a prominent strain hardening. These properties were favorable to the extrusion foaming for PP.[32,33] However, most of these works were focused on mechanical or processing properties.

It is widely acceptable that the high molecular weight component has a capability of inducing nucleation. Accordingly, whether UHMWPE will have a special influence on crystallization behaviors of the other semi-crystalline polymers is an interesting problem and has been well understood up to date, although some studies have been focused on this subject.[34–36] Feng et al. investigated the isothermal crystallization of a binary HDPE/UHMWPE blend using self-consistent mean field theory, and found that the broadening molecular weight distribution could decrease the energy barrier of nucleation and theoretically the high molecular weight component has the capability of inducing nucleation. Therefore, if UHMWPE could act as a certain nucleating agent for bimodal HDPE pipe resins and accelerate their crystallization rates.[37,38] However, there is lack of information about the effect of UHMWPE on the crystallization behavior of PP, which is very important to stabilize the extrusion foaming of PP. In this article, the nonisothermal crystallization behaviors of PP containing various amounts of UHMWPE were investigated, and prepared the PP foams containing various amounts of UHMWPE through a foaming processing under the supercritical CO_2. The aim of this article is to charity the effects of UHMWPE on the foaming properties of PP and develop the PP foams with fine cell size and high volume expansion rate through extrusion foaming with the supercritical CO_2.

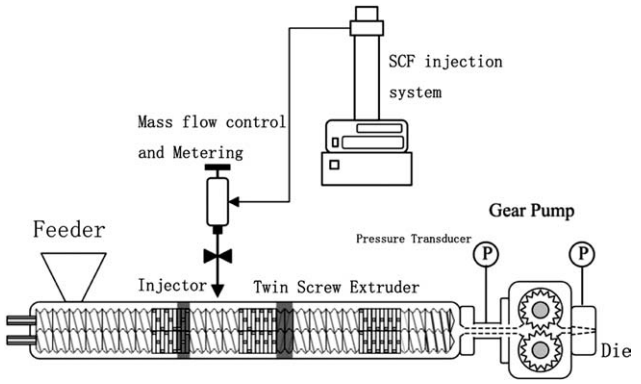

Figure 1 Scheme of the experimental equipment.

EXPERIMENTAL

Materials

Commercial PP (F401) is a conventional linear isotactic PP with a melt flow index of 2.0 g/10min and a density of 0.91 g/cm^3. It was purchased from Panjin Petro-Chemical Co., China. The UHMWPE with a viscosity average molecular weight and density of 2.0×10^6 and 0.93 g/cm^3, respectively, was kindly supplied by Beijing No.2 Auxiliary Agent Company, China. CO_2 as a blowing agent, with a purity of 99.5%, was purchased from Beijing Oxygen Co., China.

Experimental setup

Figure 1 shows a schematic of the experimental foaming extrusion system used in our study, which consists of a corotating twin-screw extruder (ZSK25-WLE, Werner & Pfleider, Germany) with a mixing screw of 30 : 1 L/D ratio, a piston pump with the flow control/metering system (designed by our laboratory), a melt pump (Extrex 28-4 SP, Magg, Switzerland), and a rapid-pressure-drop nozzle die with a diameter of 2 mm and a land length of 10 mm. A temperature transducer was installed to measure the temperature of the flowing polymer melt for precise control of its temperature at 150°C, and a pressure transducer was installed to measure the pressure of polymer melt before exiting the die.

Processing procedure

The PP and UHMWPE pellets, mixed with 1 wt % talc (only used for the foaming samples) and the other additives, were first dry blended. The mixtures were fed into the barrel through the hopper and were completely melt blended by the twin-screw extruder. The temperatures of the barrel were set from 150 to 210°C, and the screw speeds was fixed at 200 rpm. In all experiments, the amount of injected CO_2 was maintained at 7.5 wt % of the solid materials. A metered amount of CO_2 was then injected into the extrusion barrel by a SCF injection system at a given weight percentage and mixed with the polymer melt stream. When the gas was injected into the extrusion barrel, the remaining section of the twin-screw generated a shear field to completely dissolve the gas in the polymer melt via convective diffusion. The single-phase polymer/CO_2 solution went through the melt pump and was fed into the die, and the foaming occurred at the exit of the die.

Characterizations

Differential scanning calorimetry (DSC) were performed using a Perkin-Elmer PYRIS-1 differential scanning calorimeter at a scanning rate of 10°C/min to obtain the melt temperature (T_m) and enthalpy of fusion (ΔH), and to investigate the nonisothermal crystallization behavior of the foamed samples. The temperature was calibrated with indium, and about 10 mg sample was weighted very accurately. To reveal the nonisothermal crystallization kinetics, the samples were first heated to 260°C with 40°C/min, held there for 5 min, and then cooled to 50°C with the cooling rate of 10°C/min so as to erase the thermal and processing history. All DSC measurements were carried out under the nitrogen atmosphere. Wide-angle X-ray scattering (WAXS) measurement was carried out by a Rigaku D/max-r C diffractometer (40 kV, 50mA) with Cu Kα rad iation ($\lambda = 0.154$ nm), and diffraction patterns were collected in the 2θ ranges from 5 to 35°C at a scanning rate of 5°C/min.

Scanning electron microscopy (SEM) was performed using a Cambridge Stereoscan 250MK3 scanning electron microscope. The foamed samples were frozen in liquid nitrogen and then fractured to expose the cellular morphology. The fractured surfaces were then sputter-coated with a thin layer of gold, and the microstructure was observed using the SEM. The cell density (the number of cells per unit volume of unfoamed polymer) and mean cell diameter were determined on the basis of the SEM images. The two structural foam parameters were calculated using a software program (Image-Pro® Plus V6.0, Media Cybernetics). The number of cells per unit volume (N_0) of the foamed samples is determined from:

$$N_0 = \left[\frac{nM^2}{A}\right]^{\frac{3}{2}}\left[\frac{1}{1-V_f}\right] \quad (1)$$

where n is the number of cells in the SEM image; M, the magnification of the image; A, the area of the image; and V_f , the void fraction of the foamed sample. The void fraction is defined as

$$V_f = 1 - \frac{1}{\varphi} = 1 - \frac{\rho_f}{\rho} \quad (2)$$

where ρ and ρ_f is the density of the unfoamed and foam materials, respectively, and φ, the volume

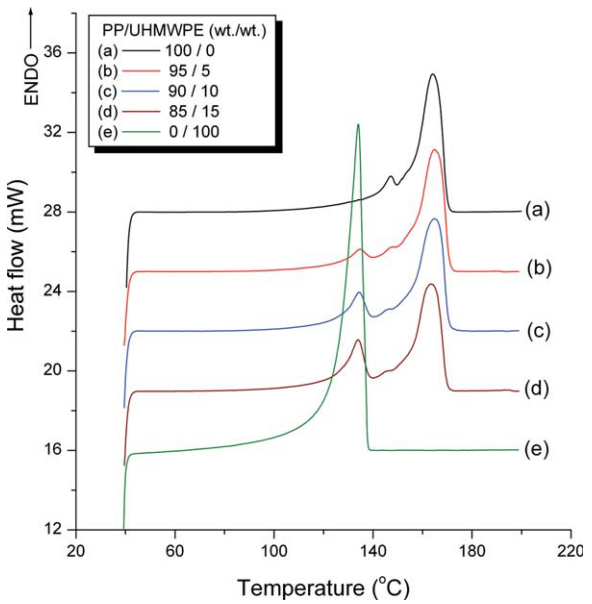

Figure 2 DSC heating thermograms of PP, UHMWPE, and the PP containing various amounts of UHMWPE. [Colour figure can be viewed in the online issue, which is available at wileyonlinelibrary.com.]

expansion rate. The digital images used to estimate the cell density and mean cell size were loaded in the software, and the image scale-bar was used to program the calibration. The mean cell diameter was measured by manually drawing the mean diameter to a minimum of 100 cells.

RESULTS AND DISCUSSION

Thermal analysis

The melt behaviors of the samples were investigated using DSC. The heating thermograms are illustrated in Figure2, and T_ms and ΔHs obtained from DSC analysis were summarized in Table I, in which ΔHs were normalized to the weight percents of the PP and UHMWPE phases in blends, respectively. As shown in the thermogram of PP, an intensive melting peak appearing at 163.1°C is attributed to the monoclinic α-PP crystal, whereas a small shoulder characterizes the trigonal β-crystal melting at 146.1°C. The UHMWPE exhibit a sole intensive melting peak at 134.0°C.[39] The thermal data confirm a high crystallinity for both PP and UHMWPE with ΔHs of 98.87 and 163.41 J/g, respectively. For the PP containing 5 wt % UHMWPE, the melting peak, appearing in the DSC thermograms at around 134.8°C, corresponds to the melting of crystallized UHMWPE, and the peak at 164.7°C is attributed to the melting of the crystallized α-PP in the blend. A slight improvement in the T_m and ΔH of the PP phase is observed as UHMWPE content increases. This suggests that the UHMWPE phase has a α-nucleating effect on the crystallization of the PP phase in the blend, which enhances the α-PP crystal.[40,41] However, the β-PP melting peak weakens, because the β-PP may easily transfer to α-PP due to the effect of the second component.[42,43] For the PP containing small amounts of UHMWPE, although the molten UHMWPE does not easily flow due to its extremely high viscosity, some of PP chains can still penetrate into the UHMWPE domains. This interferes in the crystallization of the UHMWPE chains, and thus results in a significant decrease of ΔH of the UHMWPE phase.

Crystallography

The crystallography of PP, UHMWPE and the PP containing various amount of UHMWPE was investigated by WAXS measurement, and their patterns were present in Figure 3. PP exhibited a crystallization form with the reflection appeared at $2\theta = 13.9°$, 16.7°, 18.4°, 20.9°, and 21.7° corresponding to the plane (110), (040), (130), (131), and (111) of the α-crystal phase of PP. The reflection at $2\theta = 15.9°$ was corresponding to the plane (300) of the β-PP.[44] On the other hand, it is found from Figure 3, that the WAXS profile of pure UHMWPE displays an orthorhombic crystal structure with corresponding reflex positions at 21.4° and 23.8°. From the WAXS pattern of the PP containing UHMWPE, the presence of UHMWPE does not affect the crystal structure of the

TABLE I
Thermal Analysis Data from the Heating Thermograms of PP, UHMWPE and the PP Containing UHMWPE

Sample PP/UHMWPE (wt/wt)	T_m (°C)		ΔH[a] (g/J)	
	PP phase	UHMWPE phase	PP phase	UHMWPE phase
100/0	163.14	–	98.87	–
95/5	163.77	134.80	99.95	59.08
90/10	164.95	134.24	108.74	90.47
85/15	164.86	134.01	115.73	102.01
0/100	–	134.02	–	163.41

[a] The values of ΔH were normalized to the amounts of the PP and UHMWPE respective phases in the blends.

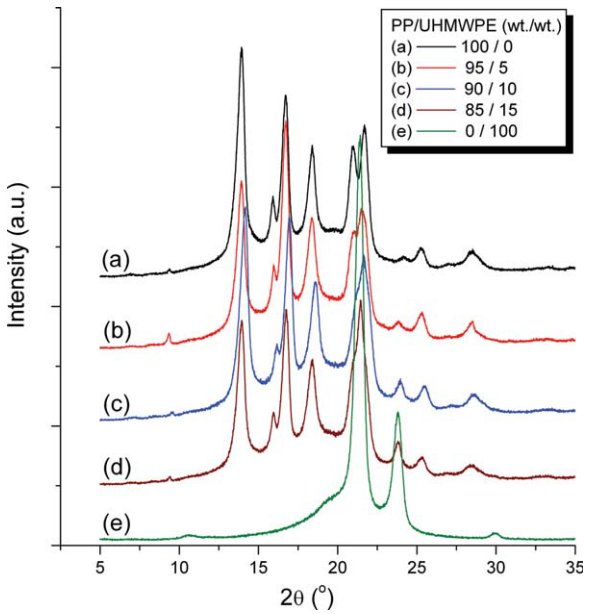

Figure 3 WAXS patterns of PP, UHMWPE, and the PP containing various amounts of UHMWPE. [Colour figure can be viewed in the online issue, which is available at wileyonlinelibrary.com.]

PP phase, though the intensity of the diffraction peak of β-PP decrease slightly and that of α-PP increases with increasing of the UHMWPE content. However, the diffraction peak at 23.8 for the UHMWPE crystal phase in blends almost disappeared, whereas an intensive peak at 21.4° overlapped by the reflection (130) of α-PP still remains. This result indicates that the crystallinity of the UHMWPE phase is diminished significantly. It is understandable that the PP crystals form at a high temperature, at which the UHMWPE phase is still in melt state; therefore, the PP-crystal phase quenches the crystallization of UHMWPE, and thus results in the depression of the crystallinity of UHMWPE phase.

Nonisothermal crystallization

The effects of UHMWPE on the crystallization behavior of PP were analyzed quantitatively through nonisothermal DSC experiments. Figure 4 displays the cooling thermograms of pure PP and the PP containing various amount of UHMWPE at selected cooling rates of 5, 10, 15, and 20°C/min. From these thermograms, the onset temperature (T_{onset}), peak temperature (T_p), and end temperature (T_{end}) for crystallization, and the temperature at the half-time ($T_{1/2}$) of crystallization can be determined, and the enthalpy of crystallization (ΔH_c) can also be obtained. These results are summarized in Table II. It is clear that the T_p, at which the crystallization rate is maximum, shifts to a lower temperature region as the cooling rate increases, while a similar trend in T_{onset}, and

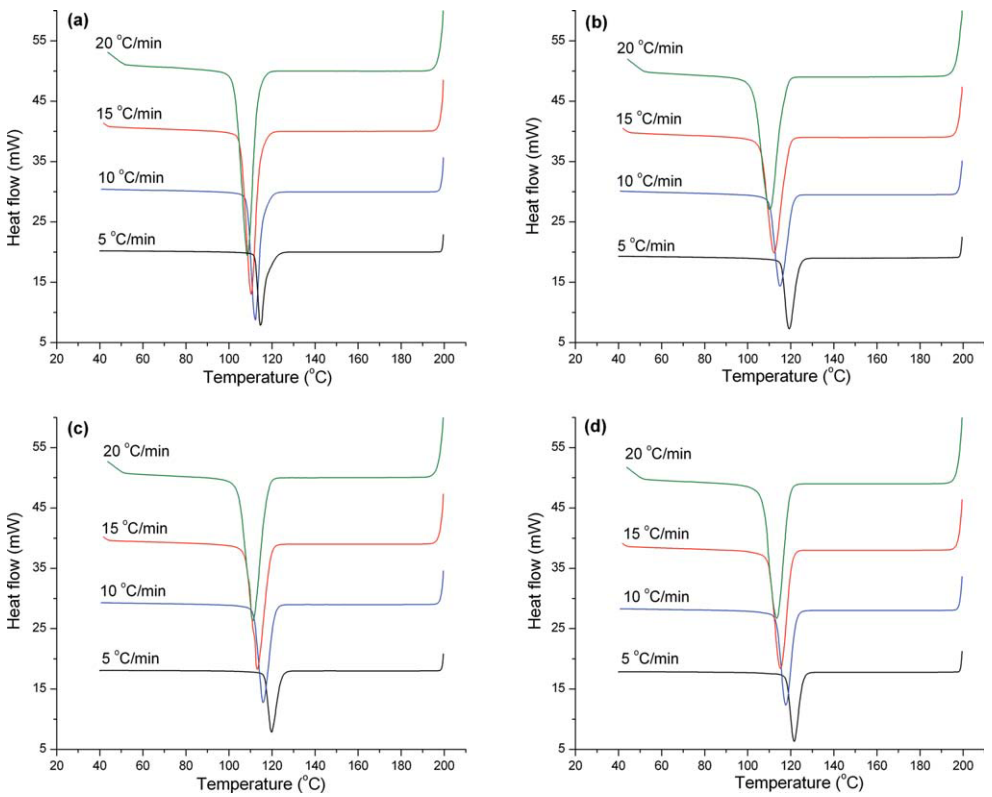

Figure 4 Nonisothermal crystallization DSC thermograms for (a) pure PP, (b) 5 wt % UHMWPE in PP, (c) 10 wt % UHMWPE in PP and (d) 15 wt % UHMWPE in PP. [Colour figure can be viewed in the online issue, which is available at wileyonlinelibrary.com.]

TABLE II
Characteristic Temperatures and Enthalpies of Nonisothermal Crystallization from the Cooling Thermograms of Pure PP, and the PP Containing UHMWPE

Sample PP/UHMWPE (wt/wt)	Cooling rate (°C/min)	T_{onset} (°C)	T_p (°C)	T_{end} (°C)	$T_{1/2}$ (°C)	ΔH_c (J/g)
100/0	5	128.5	114.6	99.6	115.3	98.4
	10	126.2	112.3	95.3	112.3	96.72
	15	124.4	110.4	93.7	110.3	95.2
	20	121.0	108.6	93.8	108.4	93.7
95/5	5	130.3	119.3	98.9	119.5	93.4
	10	126.7	114.9	96.4	115.3	90.9
	15	125.3	112.3	92.6	112.3	89.9
	20	123.5	110.2	89.0	109.7	89.3
90/10	5	132.1	119.8	91.5	120.0	93.4
	10	128.9	115.9	91.0	116.1	90.9
	15	126.4	113.2	94.5	113.3	88.9
	20	125.3	111.2	88.9	111.1	87.9
85/15	5	133.4	121.6	88.1	121.5	87.0
	10	129.8	117.7	90.3	117.5	84.5
	15	127.3	115.2	90.6	115.0	82.8
	20	126.4	113.5	89.5	113.1	81.3

$T_{1/2}$ is also observed. This phenomenon is typical for most semicrystalline polymers while crystallizing nonisothermally. When the polymer crystallizes at a low cooling rate, it has a reasonably long time remaining within the temperature range, during which a sufficient mobility of segments is promoted for the growth of crystallization. When cooled at comparatively rapid rate, the segments are frozen before the formation of regular crystallite, thereby decreasing the crystallization temperature. However, when UHMWPE was incorporated into PP, T_p and the other characteristic crystallization temperatures increase significantly at a given cooling rate, which implies that the introduction of small amounts of UHMWPE could promote the crystallization capability of PP by shortening the inducing time. It is believable that the UHMWPE molecules essentially act as an effective nucleating agent for the PP phase and increase the crystallization rate of PP during the nonisothermal crystallization. On the other hand, when much more UHMWPE is incorporated into PP, the immiscibility of the two polymers causes interference between their chains, which results in a depression of the crystallinity of the PP phase, and thus a reduction of the ΔH_c.

Figure 5 Shows the plots of relative crystallinity [$X(T)$] versus temperature (T) for pure PP and the PP containing various amounts of UHMWPE at the selected cooling rates. Here $X(T)$ as a function of T is estimated from eq. (3):

$$X(T) = \frac{\int_{T_0}^{T} (dH_c/dT)dT}{\int_{T_0}^{T\infty} (dH_c/dT)dT} \tag{3}$$

where T_0 is the initial crystallization temperature; T and T_∞, the crystallization temperature and the ultimate crystallization temperatures, respectively; and dH_c, the enthalpy of crystallization released during an infinitesimal temperature range dT.

It is well known that the Ozawa's theory has been used successfully to describe the nonisothermal crystallization kinetics of polymers.[45] Assuming that the polymer melt was cooled at a constant rate, and the mathematical derivation of Evans was valid, Ozawa modified the Avrami equation to the nonisothermal situation. According to Ozawa's theory, the relative crystallinity $X(T)$ at a crystallization temperature (T) can be calculated as:

$$1 - X(T) = \exp\left(-\frac{K(T)}{\lambda^m}\right) \tag{4}$$

where λ is the cooling rate; m, the Ozawa exponent, which is similar to the Avrami exponent to some extent and depends on the type of nucleation and growth dimensions, and $K(T)$, the function of cooling crystallization related to the overall crystallizing rate that indicates how fast the crystallization proceeds is. The above equation can also be written in another expression as:

$$\lg\{-\ln[1 - X(T)]\} = \lg K(T) - m \lg \lambda \tag{5}$$

However, many factors are not taken into account in this theory. For example, the secondary crystallization and the dependence of fold length on temperature are ignored, and the exponent m is assumed to be a constant independent of temperature. If this equation correctly describes the kinetics of nonisothermal crystallization, the plot of lg{–ln[*1*–$X(T)$]} against lgλ should give a straight line. The kinetic parameter $K(T)$ and Ozawa exponent m should be

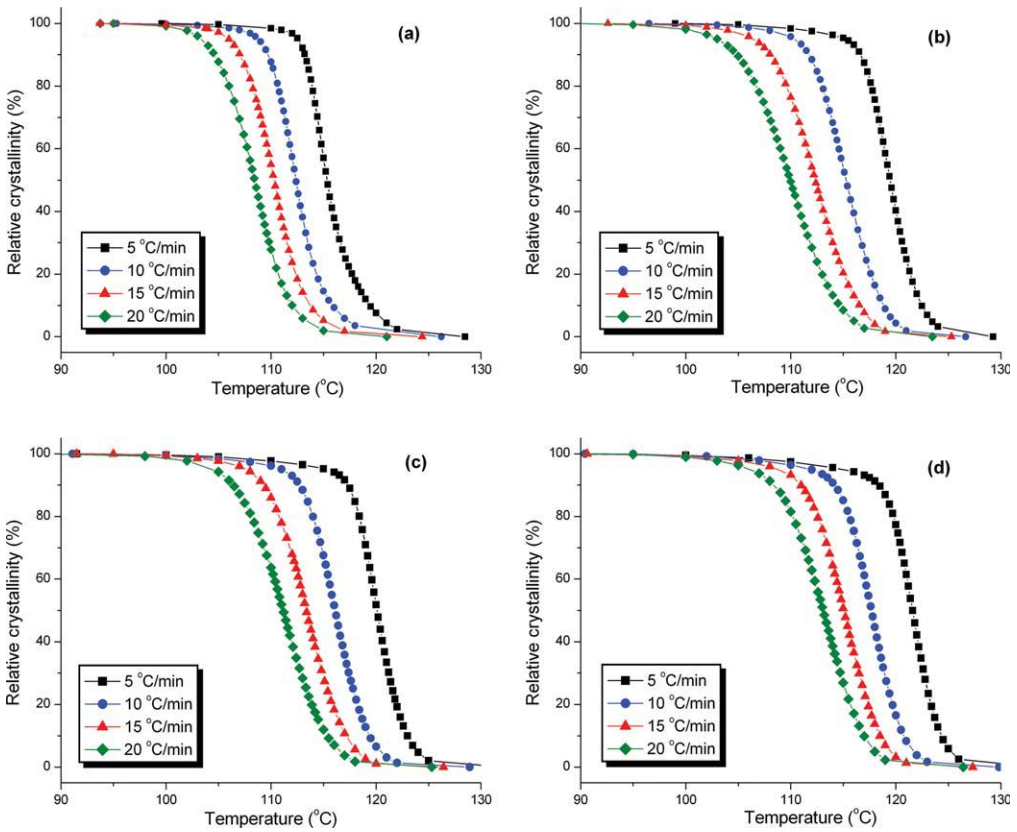

Figure 5 Dependence of the relative crystallinity on crystallization temperature for the nonisothermal crystallization at the selected cooling rate; (a) pure PP, (b) 5 wt % UHMWPE in PP, (c) 10 wt % UHMWPE in PP and (d) 15 wt % UHMWPE in PP. [Colour figure can be viewed in the online issue, which is available at wileyonlinelibrary.com.]

obtained from the intercept and the slope of the line, respectively. Figure 6 shows the plots of $\lg\{-\ln[1-X(T)]\}$ versus $\lg\lambda$ at the selected temperatures in terms of eq. (5) for the nonisothermal crystallization data of pure PP and the PP containing various amounts of UHMWPE. In our study, the Ozawa plots of pure PP complied with a good linearity when the cooling rate varies from 5 to 20 K/min. This means that an accurate analysis for pure PP of nonisothermal crystallization data could be performed with Ozawa's theory. However, the plots of the PP containing various amounts of UHMWPE exhibited a deviation from linearity, which indicating that Ozawa's equation is not appropriate to describe the nonisothermal crystallization of the PP containing UHMWPE. This suggests that Ozawa's equation [eq. (5)] may ignore the secondary crystallization deduced by the nucleation of the UHMWPE phase in blends.[46]

It is obvious that the Ozawa's equation was proven to fail to adequately describe the nonisothermal crystallization kinetics for the PP containing UHMWPE, in which the further perfection of crystal occurs. To analyze the nonisothermal crystallization for these materials better, a modified method proposed by Mo and his coworkers[47] was adopted to deal with nonisothermal data by combining Avrami's equation with Ozawa's equation. As the crystallinity is related to the λ and the crystallization time (t), the relationship between λ and t could be defined for a given crystallinity. During the nonisothermal crystallization process, the relation between the t and the T is given by $t = (T_0-T)/\lambda$, Consequently, this new kinetic equation for nonisothermal crystallization was as follows:

$$\ln\lambda = \ln F(T) - \alpha \ln t \tag{6}$$

where the parameters $F(T) = [K(T)/k]^{1/m}$, k, the crystallization kinetic constant and α, the ratio of the Avrami exponent n to Ozawa one m, i.e., $\alpha = n/m$. $F(T)$ refers to the cooling rate chosen at unit crystallization time when the system amounted to a certain crystallinity. The smaller the value of $F(T)$ is, the higher the crystallization rate becomes. Therefore, $F(T)$ has a definite physical and practical meaning to determine the cooling rate to achieve a certain crystallinity.[48]

In terms of Mo's equation [eq. (6)], the plots of $\ln\lambda$ versus $\ln t$ at the selected crystallinity should give a straight line with an intercept of $\ln[F(T)]$ and a slope of α if Mo's theory is valid. Figure 7 presents these

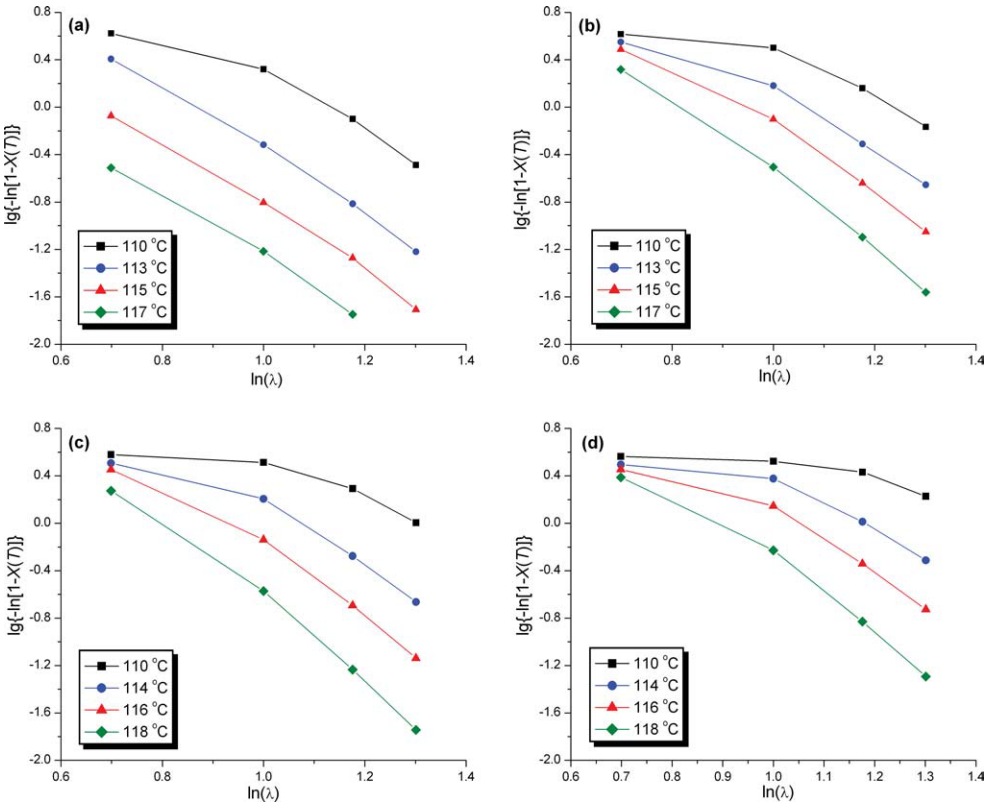

Figure 6 Ozawa's plots of lg{–ln[*1–X*(*T*)]} versus lgλ for the nonisothermal crystallization at the selected crystallization temperature; (a) pure PP, (b) 5 wt % UHMWPE in PP, (c) 10 wt % UHMWPE in PP and (d) 15 wt % UHMWPE in PP. [Colour figure can be viewed in the online issue, which is available at wileyonlinelibrary.com.]

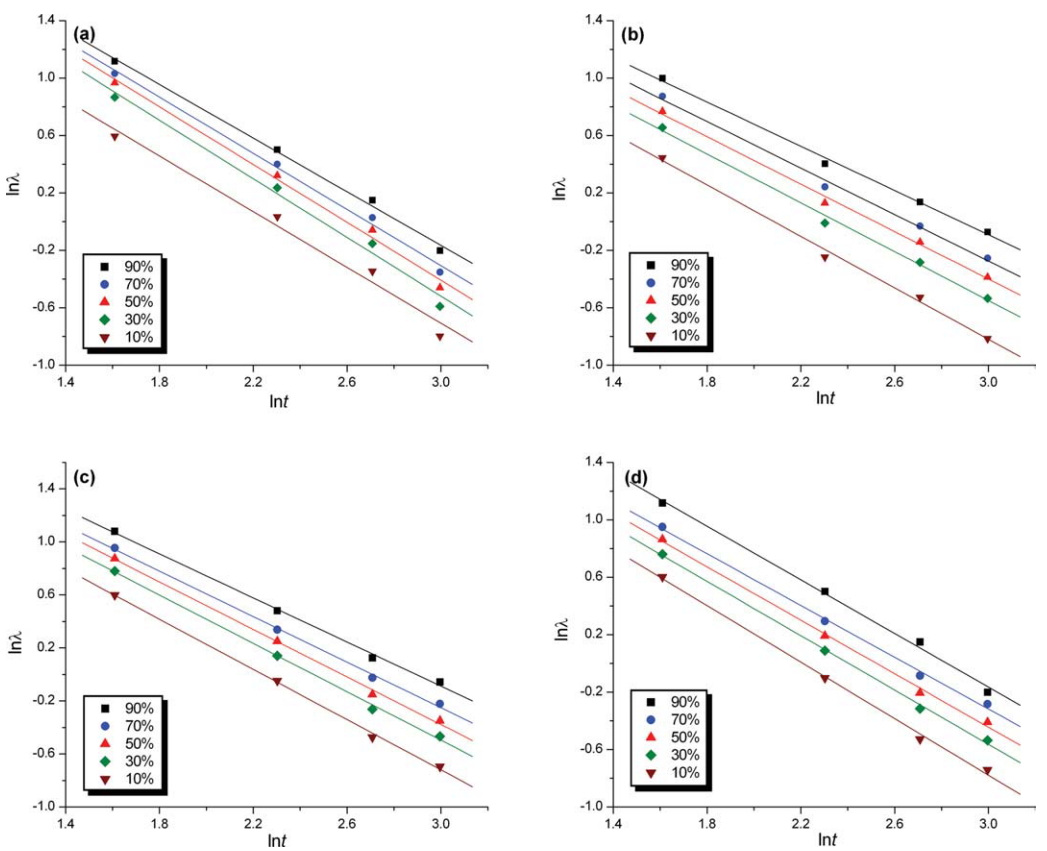

Figure 7 Mo's plots of lnλ versus ln*t* for the nonisothermal crystallization at the selected relative crystallinity; (a) pure PP, (b) 5 wt % UHMWPE in PP, (c) 10 wt % UHMWPE in PP and (d) 15 wt % UHMWPE in PP. [Colour figure can be viewed in the online issue, which is available at wileyonlinelibrary.com.]

TABLE III
Crystallization Kinetic Parameters Obtained from Mo's Equation and Activation Energies Obtained from Kissinger's Equation for the Nonisothermal Crystallization of Pure PP, and the PP Containing UHMWPE

Sample PP/UHMWPE (wt/wt)	Relative crystallinity (%)	α	$F(T)$	ΔE (kJ/mol)
100/0	10	1.303	9.69	290.49
	30	0.979	12.09	
	50	0.993	13.40	
	70	1.022	14.68	
	90	1.070	16.83	
95/5	10	1.116	8.05	198.04
	30	1.176	10.53	
	50	1.210	12.38	
	70	1.235	14.30	
	90	1.298	17.85	
90/10	10	1.056	9.39	208.86
	30	1.095	11.67	
	50	1.115	13.19	
	70	1.165	15.00	
	90	1.202	18.06	
85/15	10	1.015	9.11	248.09
	30	1.056	11.06	
	50	1.074	12.46	
	70	1.108	14.11	
	90	1.123	16.98	

plots for pure PP and the PP containing various amounts of UHMWPE, from which the values of α and $F(T)$ can be obtained from the slopes and intercepts by fitting the linearity of the eq. (6), as listed in Table III. It is notable that these plots demonstrate a good linear relationship in the range of the selected crystallinity, which indicates that the Mo's theory is successful in describing the nonisothermal process in this study, and this kinetic approach is reasonable and applicable for the PP containing various amounts of UHMWPE. The values of $F(T)$ systematically increase with an increase of the crystallinity for all the samples, but the values of α increase slightly, which indicates a slow crystallization rate is needed to reach a high crystallinity within unit time. It is interesting that the incorporation of UHMWPE into PP results in a significant depression of the $F(T)$ at a given crystallinity, and in succession, the $F(T)$ begins to increase as the amount of UHMWPE increases continuously. Here, $F(T)$ mainly reflects the crystallization facilitation to a certain crystallinity by the effect of the UHMWPE phase. The depression of $F(T)$ in the presence of UHMWPE indicates that the PP can achieve the same crystallinity faster than the pure one at a low crystallinity (i.e., lower than 70 %), which is resulted from the nucleating effect of the UHMWPE phase. However, when the content of UHMWPE increases, its super-long chains result in an entanglement with the PP chains. This effect hinders the transport of the molten PP chains to the crystal growth surface, and accordingly the crystallization rate lowers. Furthermore, the entanglement also reduces the crystal growth dimension, which is reflected by a depression of the values of α. These results indicate that the incorporation of UHMWPE may not change the nucleation type and the geometry of growing crystals of the PP phase.[49]

It is known that the crystallization process of polymers is controlled by two factors: one is the dynamic factor related to the activation energy (ΔE) for the transport of crystalline units across the phase; the other is the static factor corresponding to the free energy barrier for nucleation.To obtain the reliable values of the effective ΔE on the melt cooling process, the Kissinger's equation can be employed to determine this important parameter by considering the T_p as a function of the λ, and the ΔE of nonisothermal crystallization can be deduced as follows[50,51]:

$$\frac{d\left(\ln\frac{\lambda}{T_p^2}\right)}{d\left(\frac{1}{T_p}\right)} = -\frac{\Delta E}{R} \tag{7}$$

where R is the universal gas constant, and the other parameters have been mentioned previously. Figure 8 illustrates the plots of $\ln(\lambda/T_p^2)$ versus $\ln(1/T_p)$ for pure PP and the PP containing various amounts of UHMWPE, from which the values of $-\Delta E/R$ can be obtained by fitting the linear slopes. Accordingly, ΔE can be calculated, and the results are also listed in Table III. Since the entropy of a system decreases while transforming the molten fluid in the disordered state into the order crystalline one, the value

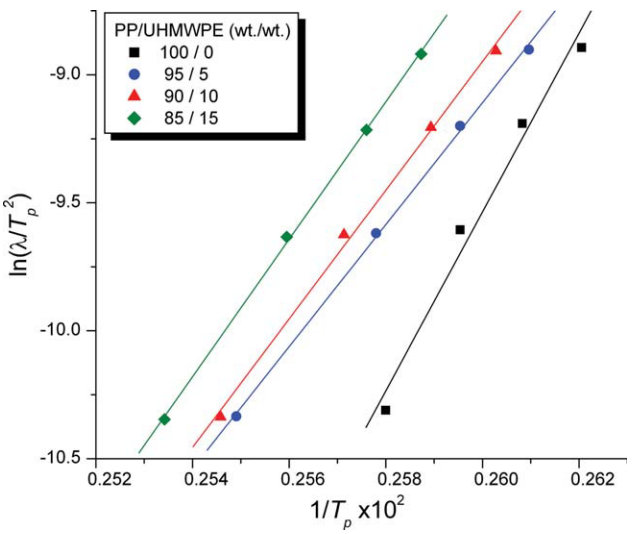

Figure 8 Kissinger's linearity-fitting plots of $\ln(\lambda/T_p^2)$ versus $\ln(1/T_p)$ for the nonisothermal crystallization of pure PP and the PP containing various amounts of UHMWPE. [Colour figure can be viewed in the online issue, which is available at wileyonlinelibrary.com.]

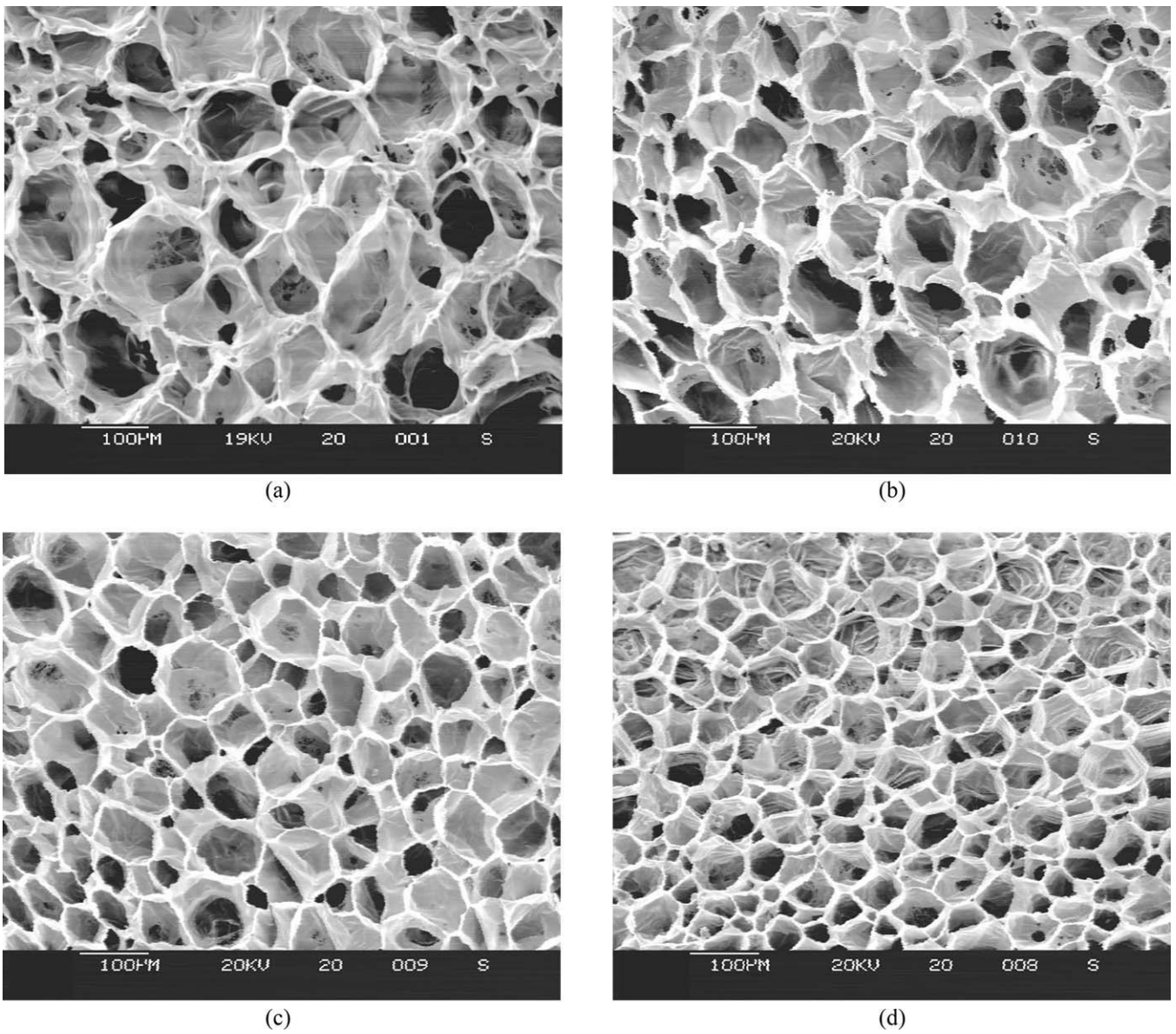

Figure 9 SEM images of the foamed samples made of (a) pure PP, (b) 5 wt % UHMWPE in PP, (c) 10 wt % UHMWPE in PP, and (d) 15 wt % UHMWPE in PP.

of ΔE for the crystallization is positive. The values of ΔEs for the PP containing UHMWPE decrease remarkably in comparison with that of pure PP, indicating that the nucleating effect of UHMWPE improves the crystallization ability of PP. Moreover, the value of ΔE begins to increase when the UHMWPE content increases. This result suggests that the entanglement caused by UHMWPE generate a negative effect on the crystallization of PP as discussed previously.

Foaming properties

Foaming samples of pure PP and the PP containing UHMWPE were prepared using a designed extrusion foaming setup with supercritical CO_2 as blowing agent. Figure 9 illustrates the morphologies of these foams. It is clearly visible that the pure PP foams display a large cell size and a very ununiform cell size distribution, and two distinct populations of cells differing in size were apparent. The large cells were likely to be formed in the amorphous phase of PP, while the small ones around and/or in crystalline regions. On the basis of the cell parameters obtained from the analysis of the SEM images as showed in Figure 10 and 11, it is also found that the pure PP foams have a high bulk density of 0.45 g/cm^3, a low volume expansion rate of 2.0, a large mean cell size of 114 μm, and a low cell density of 1.78×10^6 unit/cm^3. These results indicate a poor foamability of the pure PP. However, the SEM images reveal that the cell size is reduced, and the

uniformity of the cell size is improved with the introduction of UHMWPE. This positive effect on the cell quality is so significant that the PP foams containing 15 wt % UHMWPE exhibits an optimal small cell size with a narrow size distribution in visible region. Figure 10 and 11 also show that the bulk density and mean cell size of the foamed materials are reduced remarkably, whereas there is a prominent improvement in the volume expansion rate and the cell density with an increase of the UHMWPE content. It is observed that, when 15 wt % UHMWPE was incorporated into PP, the foams achieved a bulk density of 0.029 g/cm^3, a volume expansion rate of 31.8, a mean cell size of 40 μm, and a cell density of 1.36×10^7 unit/cm^3. These results imply that the foaming properties of the modified PP materials are improved significantly.

It is undoubted that the crystallization behavior of semicrystalline materials like PP is one of the critical factors that affect the foaming properties. During the foaming extrusion process of PP with supercritical CO_2, the melt solidifies at the moment of crystallization when cooling, and the foam structure is frozen in this stage. If the crystallization of the pure PP occurred in the primitive stage of foaming, the foam cannot be fully expanded before the dissolved CO_2 fully diffused out and in the nucleated cells, Therefore, to achieve the optimized forming properties of the PP foams, we have to make the crystallization (or solidification) occur after all the dissolved gas diffuses out into the nucleated cells. Owing to its low melt strength and narrow processing window (narrow temperature range during crystallization), the PP melt solidified too quickly before the foam was expanded fully if the processing temperature was too close to the crystallization temperature.

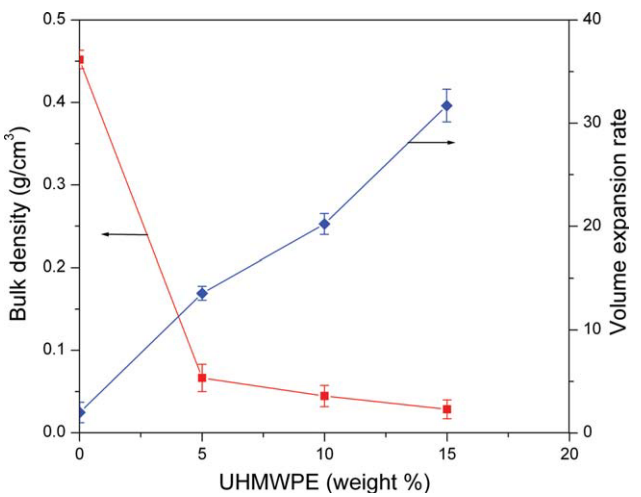

Figure 10 Bulk density and volume expansion rate of the foamed samples as a function of UHMWPE content. [Colour figure can be viewed in the online issue, which is available at wileyonlinelibrary.com.]

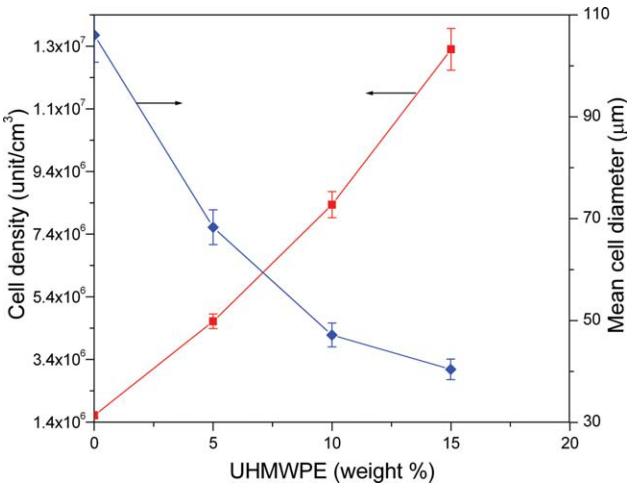

Figure 11 Cell density and mean cell diameter of the foamed samples as a function of UHMWPE content. [Colour figure can be viewed in the online issue, which is available at wileyonlinelibrary.com.]

However, if the temperature was too high, the solidification time was too long, the gas that had diffused out of the PP melt to the nucleated cells would easily escape out of the foams. As discussed previously, the incorporation of UHMWPE into PP can induce the crystallinity of PP through nucleating effect and change the crystallization course by a long-chain entanglement, which causes a variety in crystallization kinetics. It is most important that the presence of UHMWPE improves the crystallization temperature of PP and widens its temperature range during the crystallization process ($T_{onset} - T_{end}$, Table II). Compared with conversional PP, the higher crystallization temperature causes the PP/UHMWPE melt a high viscosity and thus a high melt strength at the same temperature, while the wide temperature range of crystallization makes it easy to control the foam process and improve the foam stability. These effects are beneficial to the foaming process, which can balance the gas loss and solidification (i.e., the crystallization) of PP. As a result, the foaming properties (i.e., cell uniformity and expandability etc.) were improved significantly.

CONCLUSION

A systematic investigation on the nonisothermal crystallization kinetics of conversional PP containing various amounts of UHMWPE were carried out using DSC, and the effect of UHMWPE on the crystallization behavior of the PP materials was evaluated. The kinetic studies suggested that the incorporation of UHMWPE into PP resulted in an increase in the crystallization temperature and temperature range of crystallization as well as the relative crystallinity. This behavior is ascribed to a comprehensive effect of the nucleation and

entanglement of the UHMWPE chains. The kinetic models based on Ozawa's and Mo's methods were used to analyze the nonisothermal crystallization behaviors, the former model was inapplicable to satisfactorily describe the nonisothermal crystallization behavior of the PP containing UHMWPE, whereas the method proposed by Mo and his coworkers succeeded in describing it. The activation energies for the nonisothermal crystallization determined by Kissinger's method also indicated that the crystallization ability of PP was improved with the addition of UHMWPE. The effect of UHMWPE on the foaming properties of PP demonstrated owing to the modification of the crystallization kinetics of PP by incorporating UHMWPE, the bulk density and mean cell size of their foaming materials were reduced remarkably, while the volume expansion rate and the cell density increased significantly.

References

1. Ashby, M. F.; Jones, D. R. H. Engineering Materials 2: An Introduction to Microstructures, Processing and Design; Pergamon Press: England, 1988.
2. Rodriguez, F. Principles of Polymer Systems; Hemisphere Publishing Corporation: New York, 1989.
3. Park, C. P. Polymeric Foams; Hanser: New York, 1991.
4. Klempne, D.; Frisch, K. C. Handbook of Polymeric Foams and Foam Technology; Hanser: New York, 1991.
5. Park, C. B.; Cheung, L. K. Polym Eng Sci 1997, 37, 1.
6. Naguib, H. E.; Park, C. B. Polym Eng Sci 2002, 42, 1481.
7. Liu, C.; Wei, D.; Zheng, A.; Li, Y.; Xiao, H. J Appl Polym Sci 2006, 101, 4114.
8. Sahagun, C. Z.; Gonzalez-Nunez, R.; Rodrigue, D. J Cell Plast 2006, 42, 469.
9. Naguib, H. E.; Park, C. B.; Reichelt, N. J Appl Polym Sci 2004, 91, 2661.
10. Nam, G. J.; Yoo, J. H.; Lee, J. W. J Appl Polym Sci 2005, 96, 1793.
11. Li, G.; Wang, J.; Park, C. B.; Simha, R. J Polym Sci Part B: Polym Phys 2007, 45, 2497.
12. Naguib, H. E.; Park, C. P.; Song, S. W. Ind Eng Chem Res 2005, 44, 6685.
13. Park, C. B.; Behravesh, A. H.; Venter, R. D. Polym Eng Sci 1998, 38, 1812.
14. Spitael, P.; Macosko, C. W. Polym Eng Sci 2004, 44, 2090.
15. Varma-Nair, M.; Handa, P. Y.; Mehta,, A. K.; Agarwal, P. Thermochim Acta 2003, 396, 57.
16. Xu, Z.; Jiang, X.; Liu, T.; Hu, G.; Zhao, L.; Zhu, Z.; Yuan, W. J Supercrit Fluid 2007, 41, 299.
17. Kaewmesri, W.; Rachtanapun, P.; Pumchusak, J. J Appl Polym Sci 2008, 107, 63.
18. Kaewmesri, W.; Lee, P. C.; Park, C. P.; Pumchusak, J. J Cell Plast 2006, 42, 405.
19. Kao, N.; Chandra, A.; Bhattacharya, S. Polym Int 2002, 51, 1385.
20. Liao, R.; Yu, W.; Zhou, C.; Yu, F.; Tian, J. J Polym Sci Part B: Polym Phys 2008, 46, 441.
21. Azuma, M.; Ma, L.; He, C. Q.; Suzuki, T.; Bin, Y.; Kurosu, H. Polymer 2004, 45, 409.
22. Bin, Y. Z.; Ma, L.; Adachi, R.; Kurosu, H.; Matsuo, M. Polymer 2001, 42, 8125.
23. Valenciano, G. R.; Job, A. E.; Mattoso, L. H. C. Polymer 2000, 41, 4757.
24. Okamoto, M.; Kojima, A.; Kotaka, T. Polymer 1998, 39, 2149.
25. Xie, S. B.; Zhang, S. M.; Wang, F. S.; Liu, H. J.; Yang, M. S. Polym Eng Sci 2007, 45, 1247.
26. Sugimoto, M.; Masubuchi, Y.; Takimoto, J.; Koyama, K. J Polym Sci Part B: Polym Phys 2001, 39, 2692.
27. Sugimoto, M.; Masubuchi, Y.; Takimoto, J.; Koyama, K. Macromolecules 2001, 34, 6056.
28. Wang, X.; Li, H.; Jin, R. J Appl Polym Sci 2006, 100, 3498.
29. Xie, M.; Chen, J. J Appl Polym Sci 2009, 111, 890.
30. Xie, M.; Chen, J. Eur Polym J 2007, 43, 3480.
31. Chand, N.; Naik, A. M.; Khaira, H. K. Polym Compos 2007, 28, 267.
32. Zhang, P.; Zhou, N.; Wu, Q.; Wang, M.; Peng, X. J Appl Polym Sci 2007, 104, 4149.
33. Liu, G.; Chen, Y.; Li, H. J Appl Polym Sci 2004, 94, 977.
34. Cao, W.; Wang, K.; Zhang, Q.; Du, R.; Fu, Q. Polymer 2006, 47, 6857.
35. Matsuba, G.; Sakamoto, S.; Ogino, Y.; Nishida, K.; Kanaya, T. Macromolecules 2007, 40, 7270.
36. Ogino, Y.; Fukushima, H.; Matsuba, G.; Takahashi, N.; Nishida, K.; Kanaya, T. Polymer 2006, 47, 5669.
37. Wang, J.; Wang, Z.; Yang, Y. J Chem Phys 2004, 121, 1105.
38. Wang, J.; Zhang, H.; Qiu, F.; Wang, Z.; Yang, Y. J Chem Phys 2003, 118, 8997.
39. Huang, Y.; Chen, G.; Yao, Z.; Li, H.; Wu, Y. Eur Polym J 2005, 41, 2753.
40. Wang, K.; Zhou, C. Polym Eng Sci 2001, 41, 2065.
41. Yang, Z.; Zhang, Z.; Tao, Y.; Mai, M. Eur Polym J 2008, 44, 3754.
42. Huo, H.; Jiang, S.; An, L.; Feng, J. Macromolecules 2004, 37, 2478.
43. Varga, J. J Therm Anal 1989, 35, 1891.
44. Yi, Q. F.; Wen, X. J.; Dong, J. Y.; Han, C. C. Polymer 2008, 49, 5053.
45. Ozawa, T. Polymer 1971, 12, 150.
46. Yuan, Q.; Awate, S.; Misra, R. D. K. Eur Polym J 2006, 42, 1994.
47. Liu, T.; Mo, Z.; Zhang, H. J Appl Polym Sci 1998, 67, 815.
48. Zhang, C.; Zhu, B.; Ji, G.; Xu, Y. J Appl Polym Sci 2006, 99, 2782.
49. Song, S.; Wu, P.; Ye, M.; Feng, J.; Yang, Y. Polymer 2008, 49, 2964.
50. Kissinger, H. E. J Res Natl Bur Stand 1956, 57, 217.
51. Run, M.; Wang, Y.; Yao, C.; Gao, J. Thermochim Acta 2006, 477, 13.